



# Assessing the Time Dependence of AOPs on the Surface Properties of Polylactic Acid

Charalampia Kalogirou<sup>1,2</sup> · Oliver Höfft<sup>3</sup> · Anna Gödde<sup>1</sup> · Nikolaos Papadimitriou<sup>2</sup> · Pavlos K. Pandis<sup>2</sup> · Christos Argiris<sup>1,2</sup> · Georgia Sourkouni<sup>1</sup>

Accepted: 23 September 2022  
© The Author(s) 2022

## Abstract

Plastics are artificial synthetic organic polymers that have been used in every area of daily life. However, because of their slow degradation rate, their use is contentious. The treatment of the surface of the sample is considered necessary as enzymatic or bacterial attach is not possible if the plastic surface environment is not ideal. The main topic of this work is the investigation of the effect of different advanced oxidation processes (AOP) on the near surface structure of polylactic acid (PLA) samples, which, in turn, can promote the adhesion of enzymes or bacteria for further biodegradation. The Advanced Oxidation Processes that have been used are Ultrasonication, UV photodegradation and Dielectric Barrier Discharge (DBD) plasma. After the treatments, the surfaces were characterized by Infrared Spectroscopy (IR), Drop Contact Angle (DCA), Confocal Laser Scanning Microscopy (CLSM) and X-ray Photoelectron Spectroscopy (XPS). Both ultrasonic and UV treatments have a significant impact on the surface properties of immersed PLA by removing the oxygen-containing groups of the polymer chain, albeit in different ways, while plasma tends to uncover oxygen groups on the surface. The influence of the pre-treatment on improving the adhesion of bacteria on the PLA surface has been proven using a *Pseudomonas knackmussii* strain.

**Keywords** Plastics degradation · AOPs · Ultrasonication · UV photodegradation · DBD plasma · PLA · XPS

## Introduction

Nowadays plastic pollution is one of the biggest problems due to the widespread use of plastics. Several efforts have been made to alleviate this global problem, however, the durability of plastics and their longevity led to huge waste that cannot be easily managed [1]. Strikingly, in 2015 the annual volume of plastics was equal to the volume of the total human weight on the planet [2]. Furthermore, scientists anticipate that up to 10% of all plastic waste produced will end up in the ocean, and that by 2050 plastics would

outnumber fish [3]. Plastics, and especially microplastics, can become entangled in the ecosystem and be carried to the oceans by rivers and winds [4].

Despite significant progress in understanding the behavior of microplastics in the environment because of increasing awareness and research focus, much remains unknown, particularly in terms of the ability to accurately anticipate exposure situations and identify exposure hotspots. The fate of micro/nano-plastics in the environment is difficult to predict. This is because of the many sources and channels of entry into the environment, as well as the time required to identify their degradation mechanisms.

Plastics are artificial synthetic organic polymers that have found application in every aspect of everyday life as well as in industries due to their properties, including their stability and durability. However, because of their slow breakdown rate, the use of biodegradable plastics in solid waste management is rather unclear [5, 6]. Plastics are resistant to microbial processing and in addition, there are no enzyme structures in nature capable of degrading synthetic polymers in a reasonable time. For this reason, recent attempts for

✉ Georgia Sourkouni  
cogsa@tu-clausthal.de

<sup>1</sup> Clausthal Centre for Materials Technology (CZM), Clausthal University of Technology, Leibnizstr. 9, 38678 Clausthal-Zellerfeld, Germany

<sup>2</sup> School of Chemical Engineering, National Technical University of Athens, 9 Heron Polytechniou St., Zografou Campus, 15773 Athens, Greece

<sup>3</sup> Institute for Electrochemistry, Clausthal University of Technology, 38678 Clausthal-Zellerfeld, Germany

biodegradation of polymers focuses mainly on changing their surface, enabling, and enhancing microbial adhesion.

PLA is marketed as biodegradable polymer and created the false impression that PLA can be simply landfilled to disappear although according to ASTM International D5338-1 PLA is compostable at  $58 \pm 5$  °C making PLA recalcitrant under normal conditions in landfills [7].

It has been found that complete degradation of PLA in nature can last even decades, while the degradation rate in seawater is even lower [8]. Recently Morohoshi et al. have found no biofilm formation at all in seawater [9]. No degradation of PLA in seawater is reported in a mini review by Haider et al. [10].

Therefore, pre-treatments of the polymer surfaces are considered necessary for effective microbial adhesion. These pre-treatments result in the formation of functional groups of carbonyls, carboxyls and esters [11, 12]. Mat Yasin et al. published a critical review on the enhancement of (bio)degradable bioplastics through pretreatments [13].

Aside from physical modification, polymers may be degraded using a variety of processes, including thermal degradation, photolysis, chemical procedures, microwaves, atmospheric DBD plasma and biodegradation using enzymes and bacteria [14, 15]. The majority of these reactions occur at random and produce unwanted mono- and oligomers as well as changes in the chemical microstructure of the side groups. On the other hand, it has also been reported that ultrasound is an ideal approach when reduced molecular weight products are needed [14].

Sonochemistry can be used to bring molecules of a compound to reaction, due to the application of high-power ultrasound (20 kHz–10 MHz) [15]. The chemicals resulting from ultrasonication have been studied for more than 60 years. Compared with the rest of the traditional techniques, ultrasonic radiation provides unusual reaction conditions, such as very high temperatures and pressures which cannot be achieved by other methods [16]. Several theories have been developed to explain how chemical bonds are broken, against the effect of 20 kHz ultrasound radiation. In the scientific field, it has been established that the main event that takes place in sonochemistry is the creation, development and final collapse of a bubble formed in a liquid. The diffusion of its vapours with the dissolved substance in the volume of the bubble, leads to its growth, while the collapse of the bubble occurs when its size reaches a critical value. To determine the location at which the sonochemical reaction takes place, the rates of volatile metal carbonyl substitution reactions have been studied turning out that there are two areas: one corresponding to the gas phase inside of the collapsing bubble, and one corresponding to a thin layer surrounding the cavity. Also, after the determination of the above positions, it became possible to find the effective temperature in each reaction zone. It turned out that the belts of

liquid and gaseous phase reactions, have effective temperatures of 1900 K and 5200 K, respectively. The phenomenon of the creation, growth, and eventual collapse of the bubble can be explained based on the hot spot mechanism. Based on this theory, when the bubble collapses, very high temperatures are obtained, (5000–25,000 K), and since this collapse occurs in less than 1 ns, very high cooling rates, higher than  $10^{11}$  K / s are achieved [17–19].

If one compares the impact of low frequency (20–40 kHz) and high frequency (0.6–2 MHz) ultrasounds (US), then different effects are expected to be found on the polymer surface. Low frequency US has a higher impact as the cavitations produced are bigger in diameter and thus release higher energy amounts upon their collapsing on surfaces causing mechanical but also chemical erosion. At higher frequencies the cavities are much smaller, but their number is higher and therefore more chemical than mechanical effects are expected. One speaks about softer cavitation effects at higher frequencies at the same US power as the experiment at lower frequencies. It is possible that high energy US based cavitation (low frequency) can also mechanically clean the surface and partly eliminate the produced effects making obvious the present study of time dependence of the polymer surface treatment [20].

Photochemistry studies the chemical effects of light on matter. It is known that classical chemical reactions may happen due to the influence of visible (Vis) and ultraviolet light (UV). UV is a non-mechanical energy input technique that could destroy organic compounds including water-soluble contaminants as well as solid organics and plastics. Light can decompose organic materials and is one of the primary drivers of plastic deterioration in ambient conditions, while especially the impact of ultraviolet (UVA) radiation (400–290 nm) and visible light can partly degrade the majority of synthetic polymers. This is because UVA radiation has energy ranging from 3.1 to 4.3 eV, corresponding to 72–97 kcal/mol. This implies that it has enough energy to disrupt most chemical bonds, and therefore light can function similarly to thermal deterioration [21, 22].

In recent years, Dielectric Barrier Discharge (DBD) Plasma has shown to be a viable technique for modifying the surface characteristics of polymers. The dielectric performs two important purposes in the discharge operation: first, it restricts the amount of charge that can be transferred from one electrode surface to another by a single micro-discharge, and second, it spreads these micro-discharges across the whole electrode region. Voltages of a few kV and frequencies ranging from 5 to 500 kHz are commonly utilized. The average electron energy in DBD plasma is in the 0–10 eV range, meeting the chemical binding energy of plastics, which is no more than 10 eV. Plasma modification techniques provide advantages over other treatments, such as the capacity to modify the surface evenly without affecting

bulk characteristics. This approach has been demonstrated to be a potential method for performing surface treatments on polymers without altering their bulk properties. Another advantage of DBD is the ability to alter the surface characteristics of polymers without the need for costly vacuum equipment [23, 24]. Our main focus was on how the duration of the treatment with different advanced oxidation processes affects the surface properties resp. the structure of the samples. Therefore, the samples, immersed in demineralized water, have been treated separately via UVA irradiation and ultrasonication of High Frequency Ultrasounds (HFUS) at 860 kHz and Low Frequency Ultrasounds (LFUS) at 20 kHz for 1, 3 and 6 h. In another experiment, samples have been treated with atmospheric DBD plasma in ambient air for 5, 10, 20 and 60 s. In the present manuscript, we will discuss the changes in the functional groups of PLA in the near surface region using the results of X-ray photoelectron spectroscopy and IR spectroscopy. The changes in surface morphology such as surface roughness will be presented using Confocal Laser Scanning Microscopy. In addition, the wetting behavior of the treated samples will be investigated using Drop Contour Analysis. The influence of the pre-treatment on improving the adhesion of bacteria on the PLA surface is demonstrated using a *Pseudomonas knackmussii* strain.

## Materials and Methods

### Materials

In this work polymeric samples of polylactic acid (PLA) were used, which has been the subject of research for over a century. In the beginning, PLA films (20 × 20 cm) with a thickness of around 1 mm were produced. The samples were created as the film was initially engraved on the marked points and then by applying pressure on the edges it breaks into smaller pieces. As we reported in our previously published paper [20] in the present work a commercial, semi-crystalline, bio-based polylactic acid (PLA) grade, Purapol L130 from Corbion was used for the film production by compression molding. This PLA grade has high heat properties, medium flow and higher temperature resistance (viscosity average molecular weight  $M_v = 179,000 \text{ g mol}^{-1}$ ,  $[\text{COOH}] = 7 \text{ meq kg}^{-1}$ ,  $T_g = 70 \pm 1 \text{ }^\circ\text{C}$ ,  $T_m = 180 \pm 1 \text{ }^\circ\text{C}$ , melt flow index (ISO 1133-A at 210 °C/2.16 kg) = 16 g/10 min, Melt flow index (ISO 1133-A at 190 °C/2.16 kg) = 7 g/10 min). Purapol L130 has high optical purity, containing mainly L-isomer (min.99%). As it is recommended, Purapol L130 white pellets were dried in an oven at 100 °C, for 4 h prior to processing. PLA films (15 × 15 cm) of approximately 1 mm thickness were prepared via compression molding. The material

was brought up to the molding temperature ( $190 \pm 2 \text{ }^\circ\text{C}$ ) for 7 min, molded for 8 min under  $200 \pm 1 \text{ bar}$  and then cooled down under compression to ambient temperature in ca. 10 min. The hot-pressed PLA foil was cut in samples with dimensions of  $10 \times 10 \text{ mm}^2$ .

Based on results of Sarasua et al. [25, 26] the crystallinity in thermally treated PLA foils is fully developed after 10 h treatment at 190 °C. As the foils in the present study were prepared at 190 °C for only 8 min molding time, we expect a low crystallinity in the range of less than 10%. In the second PLA-foil batch used for the plasma treatment we found that starting with a PLA crystallinity of 34% the resulting foil was practically amorphous. This, along with the cooling of the suspension of the PLA samples during all pretreatment methods at 25 °C (in order to avoid thermal changes in both the sample bulk and surface) and the use of cold plasma as already published by Song et al. [27] leads to the assumption that the bulk properties are not affected by the treatment procedure and only surface effects re observable.

### Treatment Methods

As stated above, the samples have been treated separately via UVA irradiation and ultrasonication of High (860 kHz) and Low Frequency (20 kHz) for 1, 3 and 6 h. Initially, 6 PLA samples are immersed in demineralized water. After 1 h, the experiment was stopped and 2 samples were taken out, dried under ambient conditions, and kept in a dark environment. Similarly, we took samples at 3 and 6 h of the experiment. Additional samples have been treated with atmospheric DBD plasma in ambient air for 5, 10, 20 and 60 s.

### UVA Treatments

The PLA samples were treated with UVA irradiation by immersing them in demineralized water in a UVA transparent baker and placing them on a stirring plate in the self-made UV reactor. The reactor includes three 11 W UVA lamps on each side, resulting to 66 W UVA irradiation while being stirred continuously. In the UV treatments, no photocatalytically active materials were included.

### Sonication Treatments

The ultrasonic processor UIP500hdT (20 kHz, 500 W) from Hielscher Ultrasound Technology, Germany, was used to generate low-frequency ultrasounds (20 kHz). The power intensity was set at  $100 \text{ W/cm}^2$  and delivered through a 2.2 cm diameter tip. The Ultrasound Multifrequency Generator fitted with the Ultrasound Transducer E805/T/M and an adapted glass reactor UST 02/500–03/1500 from Meinhardt® Ultrasonics, Germany, produced high-frequency ultrasound with a maximum output power of 400 W. The

frequency was set to 860 kHz, and the power amplitude was set at 40%. An external Julabo recirculating cooler set to 20 °C was used for both low and high frequency to prevent the polymers from exceeding the glass transition temperature ( $T_g$ ), which is low (about 55–60 °C) and to shield the high-frequency equipment, which can be destroyed at temperatures over 50 °C. Temperature was kept at  $25 \pm 1$  °C for ultrasonication treatments.

### DBD Plasma Treatment

The dielectric barrier discharge (DBD) reactor, which was used for the experiments, consists of two parallel stainless-steel electrodes with  $30 \times 50$  mm<sup>2</sup> dimensions and a 7 mm thick alumina ceramic plate as dielectric. For the experiments, the DBD plasma settings at ambient air were 16 kV at a frequency of 7 kHz with a spacing of 9 mm between the electrodes and the samples (including the 7 mm thick dielectric).

### In Vitro Biodegradation using *Pseudomonas Knackmussii* Strain

The pretreated PLA samples have been exposed to *Pseudomonas Knackmussii* in order to first study the PLA surface behavior regarding improved bacteria adhesion and in a following step the PLA degradation.

Therefore, PLA samples have been sterilized after their pretreatment by being dipped in 70% ethanol in a laminar flow cabinet. All nutrients and media (s. Supporting Information File) for the bacteria cultivation have been autoclaved at 121 °C and stored either at room temperature or in the refrigerator.

**Revitalization and Cultivation of the Strain *Pseudomonas Knackmussii*** In order to revitalize the strain *Pseudomonas Knackmussii*, the pellet, which includes the freeze-dried cells is diluted in 10 mL of cultivation medium (40% PM, 60% CM) and incubated at 30 °C overnight (160 rpm). The following day, 1 mL of the grown cells is diluted with 250 mL of cultivation medium. This expansion of the volume is required for the cells to grow properly. All the culture media have been prepared in the laminar flow cabinet.

**Starvation of the Strain and Biodegradation** The medium for the starvation is prepared (20% PM, 80% CM). The blank pristine PLA sample (reference) is put in a flacon with 10 mL of the prepared medium. In another flacon, 100  $\mu$ L of the cells are diluted with 10 mL of the starvation medium and the pretreated sample is put in the flacon. Both flacons are incubated for 3 weeks (250 rpm, 30 °C). Every two days 5 mL are removed from the flacon, which contains the

pretreated sample and 5 mL of fresh medium are returned. After three weeks the samples are removed.

**Visualization of the Biofilm** The reference sample is rinsed with water, ethanol and weighed. The pretreated sample is rinsed with ethanol and left to dry. Afterwards it is dipped into crystal violet solution (1 g of crystal violet powder, 50 mL of ethanol, and the total volume is adjusted to 1 L with distilled water). Then it is rinsed with 80% acetic acid, let to dry, and then weighed. It can be stated that a biofilm has been formed if the sample is mauve.

### Characterization Methods

After the treatments and in order to see how they affect the surface of the PLA, the samples were analyzed using various characterization methods. In all methods, we have performed measurements at least twice (XPS) or more times (IR and CLSM). Using X-Ray photoelectron spectroscopy (XPS) we can observe the change in the elemental surface composition, while with FTIR the concentration of the active surface groups can be estimated. Drop Contour Analysis (DCA) is used to characterize the wettability of the surface and Confocal Laser Scanning Microscopy (CLSM) to measure the surface roughness and observe the morphology of the surface, as CLSM provides 3-dimensional surface profiles, by capturing multiple two-dimensional images at various depths. Combining the results of each characterization method we are able to scrutinize how each pre-treatment method affects the surface of PLA samples, both chemically and morphologically.

### X-Ray Photoelectron Spectroscopy (XPS)

XPS spectroscopy is used for chemical analysis and identification of the chemical state of the elements on the surface of a solid. The XPS spectrum reflects the energy spectrum of the emitted photoelectrons and consists of a series of distinct responsive bands in the characteristic layers of the electronic structure of the atom [28].

The experimental investigations of the untreated and treated PLA samples were performed in a UHV chamber with a base pressure of below  $5 \times 10^{-10}$  mbar. The films were characterized by core level spectroscopy (XPS) using Al K radiation with 1486.6 eV photon energy of a non-monochromatic X-ray source (Omicron DAR 400). Emitted electrons were detected by a hemispherical analyzer (Omicron EA125) under an angle of 45° to the surface normal. The analyzer was operated with a constant pass energy of 50 eV for survey spectra and 20 eV for detail spectra. Since degradation of polymer films, that are exposed to non-monochromatic X-ray radiation, was observed before [29, 30] the XPS analysis was performed as fast detail scan of the C 1 s, O 1 s, regions

and the survey spectra with a total exposure time of about 1 h. All spectra were displayed as a function of the binding energy with respect to the Fermi level. The XPS spectra have been charge-corrected by fixing the C 1 s component of the aliphatic C–C/C–H group to 285.0 eV. For quantitative XPS analysis, a Tougaard-background-subtraction was employed. Photoelectron peak areas were calculated by fitting Gauss-Lorentz type profiles optimized by the Levenberg-Marquard algorithm with the CasaXPS software. Photoelectric cross-sections calculated by Scofield [31] and asymmetry factors calculated by Yeh and Lindau [32] as well as the transmission function of the hemispherical analyzer have been considered for stoichiometric calculations.

### Confocal Laser Scanning Microscopy (CLSM)

The Confocal Laser Scanning Microscopy (CLSM) measurements were performed using the microscope VK-X200K from KEYENCE. The good lateral resolution (approx. 160 nm) enables the accurate mapping of many samples. On the software side, several images can be combined to produce one large image, meaning that even when significantly enlarged, wide areas of the sample can be mapped. Because the topography of the sample is recorded, it is possible to conduct roughness analyses or profile sections. A wide field microscopic image is also captured at the same time [33, 34].

### Drop Contour Analysis (DCA)

The Drop contour analysis (DCA) measurements were performed using the Dataphysics OCA. The Dataphysics OCA enables contact angle measurements and the determination of associated material parameters under various conditions (Fig. 1). Different atmospheres, such as nitrogen or vacuum conditions ( $p_{\min} = 1$  mbar) can be configured. The temperature can vary between room temperature and 1800 °C. The video recording enables the recording of changes in the contact angle over time and the determination of the melt

temperature. Due to the geometry of the furnace, the size of the drop is limited to a diameter of approximately 2 cm [35, 36].

### Infrared Spectroscopy (IR)

The characterization of the treated PLA samples by IR spectroscopy was carried out using the Bruker ATR-FTIR-spectrometer ALPHA-T FTIR, which is coupled with an Attenuated Total Reflexion (ATR) accessory. A diamond crystal serves as the internal reflection element. The measurements were performed by pressing the sample onto the ATR-crystal. In a spectral range from 4000 to 400  $\text{cm}^{-1}$ , 16 scans with a spectral resolution of 2  $\text{cm}^{-1}$  were recorded at 5 places (corners and center) on each sample.

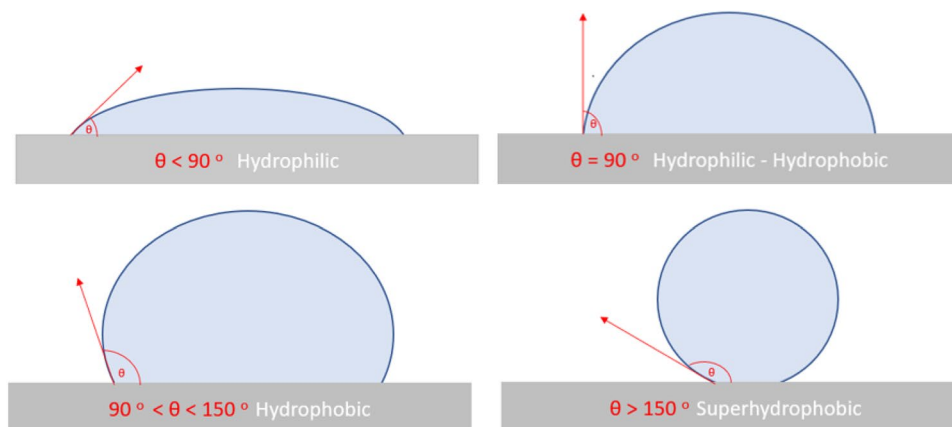
## Results

### XPS Results

The XP survey spectrum of the reference sample (Fig. 2) shows the main photoelectron peaks of carbon (C 1 s) around 285 eV and oxygen (O 1 s) around 530 eV. In some samples fluorine was detected (F 1 s peak around 690 eV) on the surface, most probably due to the production process of the PLA film samples. The spectra of the ultrasonically treated samples additionally showed nitrogen in a small percentage (<2.5%). The C 1 s and O 1 s detail spectra (Fig. 3) of the reference sample show the binding species (C–C/C–H, C–O, O=C–O) typical for PLA, whose binding energies correspond well with the literature after charge correction [28].

The respective peak areas for the individual carbon bonds do not correspond to the theoretical values for PLA of 33% per bond [28, 36, 37]. The excessive amount of C–C bonds is often observed for untreated PLA [38–40] and is likely due to unknown additives or atmospheric contaminations. Figure 4 shows the C 1 s spectra at the 20 kHz Ultrasound

**Fig. 1** Surface wetting characterization by the values of contact angle



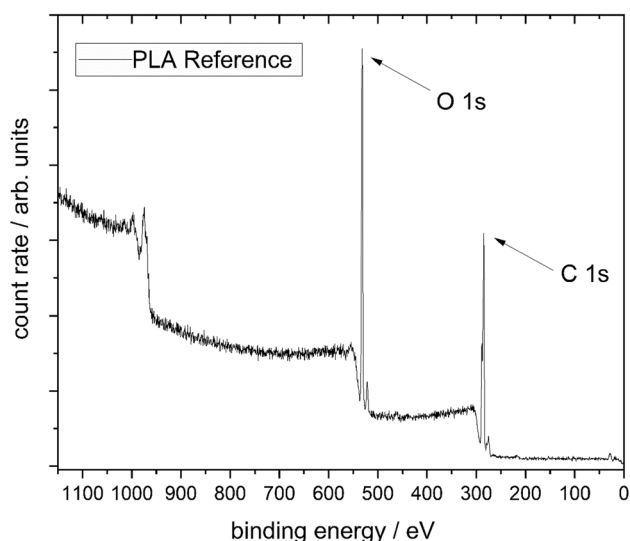


**Fig. 2** XPS survey spectra of the Reference PLA sample, showing the characteristic peaks for Carbon and Oxygen

treatment comparing the samples that have been treated to the reference sample. The percentages of the respective bonding types (C–C/C–H, C–O, O=C–O) were evaluated for each spectrum (presented in Fig. S1, S2 and S3 in Supporting Information File). When the samples are treated with 20 kHz, there is a slight increase in the C–C bonds and a reduction of C–O or O–C=O bonds in the PLA. However, a clear trend in time dependence cannot be identified. It looks as if the C–C content increases up to the 3-h treatment and then falls again slightly. It should be noted, however, that nitrogen is only found in the samples after a period of 3 h. In contrast to the low frequency US, the samples treated with 860 kHz show clear changes. In this case, there is a clear increase in the C–C bonds and a strong reduction in

the C–O bonds, whereby the O–C=O bonds are stronger reduced. This behaviour is also observed in the interaction of UVA radiation with the samples. There is also a strong increase in the C–C bonds and a reduction of C–O bonds in the PLA. Similar to 20 kHz, the proportion of C–C bonds varies with time without following a clear trend. However, the 6-h treatment resulted in the strongest decrease in C=O bonds. Again, nitrogen could only be observed after 3 h.

The interaction with the DBD plasma shows a different picture. The C–C bonds first increase in the first 5 s of treatment period and then decrease with further treatment time. The O–C=O- and C–O-bonds also decrease at first and then increase again, whereas the proportion of C–O-bonds after 60 s rather corresponds to the initial value (Fig. 5). However, the O–C=O bonds increase due to the plasma treatment compared to the reference. The proportions of the bonds almost correspond after 60 s to those that would be expected for a clean PLA surface [30, 38]. In this respect, the changes due to plasma treatment are reinterpreted in contrast to our previous publication [23]. As already mentioned above, many XP spectra of untreated PLA show a higher fraction of C–C bonds. Different types of air plasma treatments reduce this fraction as observed here [39–41]. This change is mostly associated with an increase in the fraction of oxygen bonds and is interpreted as an oxidation of the surface [39–41]. However, since all proportions are close to the theoretical values of pure PLA after the interaction, the observed changes could also be interpreted as a cleaning effect. To clarify this, further investigations would have to be carried out with, for example, longer treatment times and other gas atmospheres. Furthermore, the time after the plasma treatment has to be considered. For example, Song et al. observed an increase in C–C and C=O bonds after microwave plasma treatment in O<sub>2</sub> [42]. Their data suggest the formation of carboxylic acid and ethyl groups at the surface.

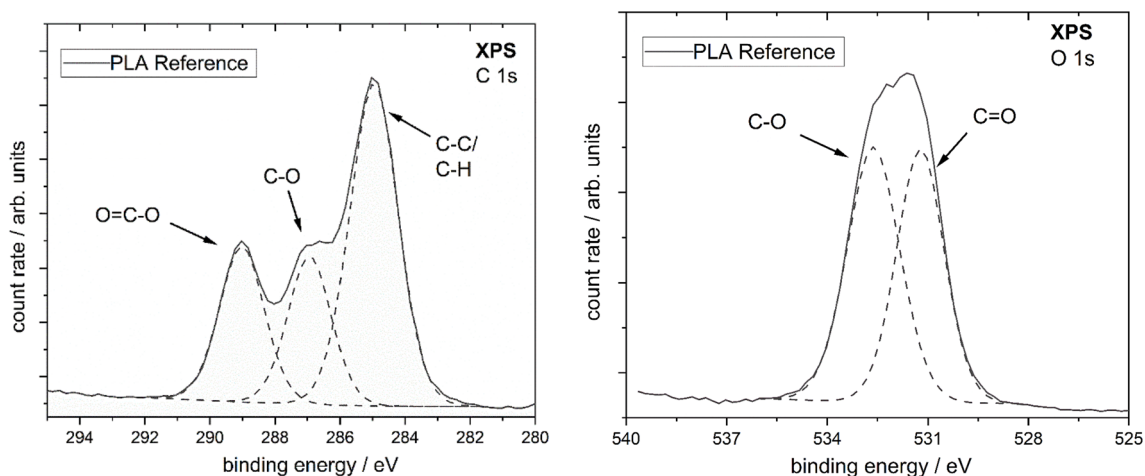


**Fig. 3** (Left) XPS Carbon peaks spectra of PLA Reference sample, (right) XPS Oxygen peaks spectra of PLA Reference sample

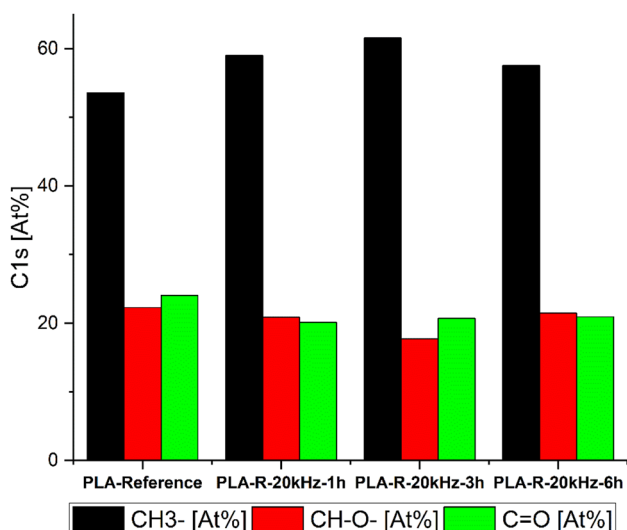


Fig. 4 C1s spectra of the 20 kHz ultrasound treated samples showing the development of the chemical composition of the surface with treatment time

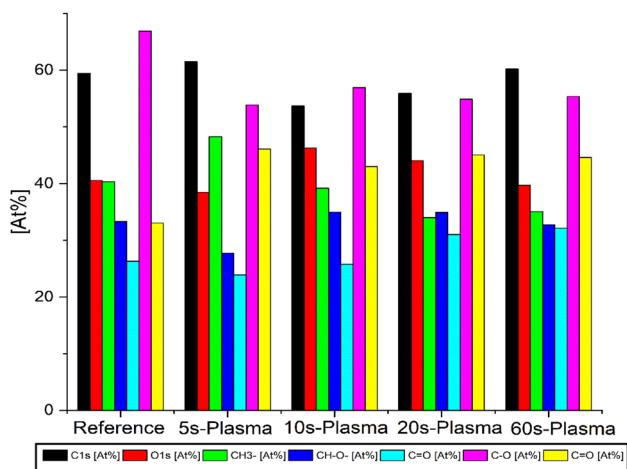


Fig. 5 The different ratios of functional groups and elements for each sample treated with plasma at different times

The comparison with results for UV treatment of PLA shows an opposite picture. The PLA that was treated here in water with UV shows a significant increase in C–C bonds. This increase also does not change with treatment time. The values differ only marginally. In contrast to the ultrasound samples, no nitrogen was observed. Ikada [43] observed an increase in C=C and carboxylic acid groups with IR spectroscopy for PLA treated with UV light in air. He attributed this to the Norrish II type photo cleavage process, where cleavage occurs at the C-O bond in PLA. This scission of the C-O bond is also the basis for the explanations of the plasma results of Laput et al. and Song et al. [41, 42]. The cleavage leads to the formation of radicals, which leads to the

formation of carboxylic acids and ethyl groups with cleavage of CO<sub>2</sub>, C<sub>2</sub>H<sub>4</sub>, and H<sub>2</sub>O [41, 42]. This clearly shows that the environment plays a major role in the interaction. However, it could be that the water dissolves compounds, like carboxylic acids, formed on the PLA surface, leaving behind a higher proportion of C–C bonds. To our best knowledge, ultrasound-assisted degradation of PLA has not yet been studied by other groups.

Comparing the 20 and 860 kHz data, it appears that the 860 kHz treatment has a much stronger influence on the PLA structure and leads to similar results as the interaction with UVA radiation due to the higher energy input. At first glance, the treatment time has little influence on the chemical composition. The strong changes could be observed already after a treatment of 1 h. To what extent or whether compounds are transferred into the water cannot yet be said.

### IR Results

The characterization of the treated PLA-samples with ATR-FTIR-spectroscopy enables the obtaining of chemical information in a range of 0,5–5 μm. The relevant peaks, which were assigned to corresponding chemical bonds, show different intensities, depending on the treatment.

For the samples that were treated with 20 kHz ultrasound, a basically increasing tendency of the intensities with an increase in duration of the treatment can be recognized (Fig. 6).

An exception are the intensities of the C = O, CH<sub>3</sub> and C-O bands of the three-hour treated sample. These are higher than those of the other samples for the first two

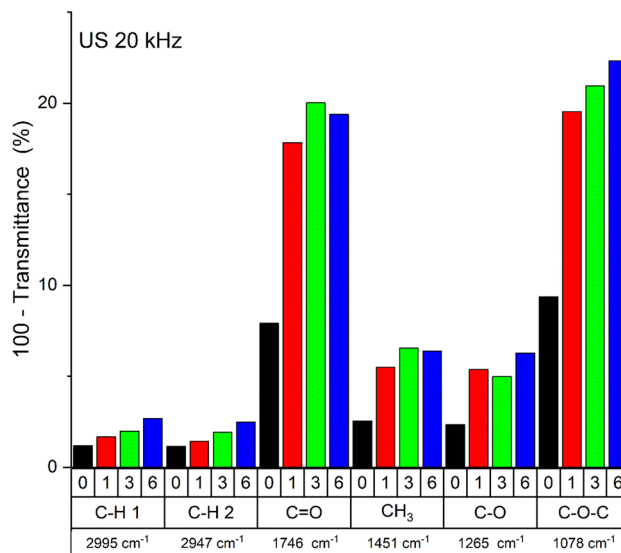


Fig. 6 Absorbance of surface groups derived from FT-IR spectra for samples treated with 20 kHz Ultrasounds. (0,1,3,6) on the X-axis indicate the treatment time in hours

cases, but the C-O peak is less pronounced than the peaks of the one- and three-hour treated samples.

The sample series treated with 860 kHz ultrasound shows only slight deviations of the intensities from the reference for both C-H-bonds (Fig. 7). These only marginal differences are also present for the six-hour treated sample. In contrast, the intensities of the C-O, CH<sub>3</sub>, C=O, C-O-C bands of the one-hour treated sample are up to 39% higher than those of the reference.

Apart from the sample irradiated for three hours, the samples treated with UV radiation show a decreasing trend in intensities (Fig. 8). Irradiation for three hours has led to a strong increase in the intensity of all bands.

Structural differences are shown only in the IR spectra of the samples treated for three hours with 20 kHz, for one hour with 860 kHz, and for one hour with UV radiation. The latter shows the formation of two small peaks at 1554 and 1509 cm<sup>-1</sup>. The first two show the formation of a new band at 1540 and 1542 cm<sup>-1</sup>, respectively. The formation of a peak in this range was already observed by Lambert and Wagner for microplastic PLA that had been naturally aged for 112 days [44]. The range between 1500 and 1600 cm<sup>-1</sup> is typically where the peaks of nitrogen compounds are found [45].

Because of the greater depth of penetration of the infrared radiation into the material, a different region of the material is imaged than, for example, in XPS spectroscopy. Accordingly, the IR spectra provide information from deeper layers of the PLA.

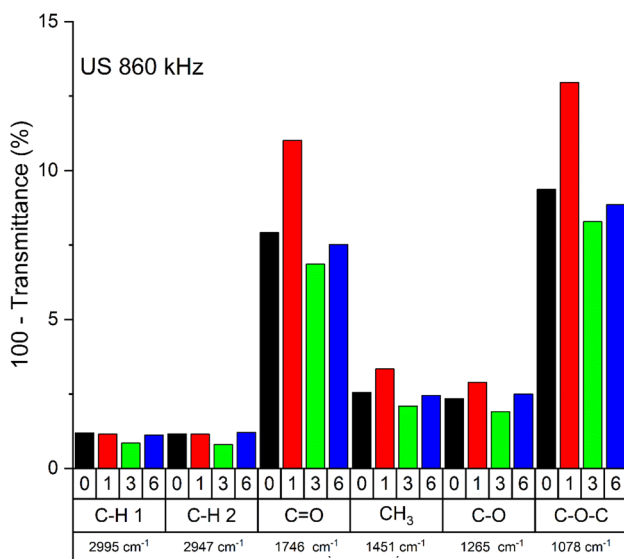


**Fig. 7** Absorbance of surface groups derived from FT-IR spectra for samples treated with 860 kHz Ultrasounds. (0,1,3,6) on the X-axis indicate the treatment time in hours

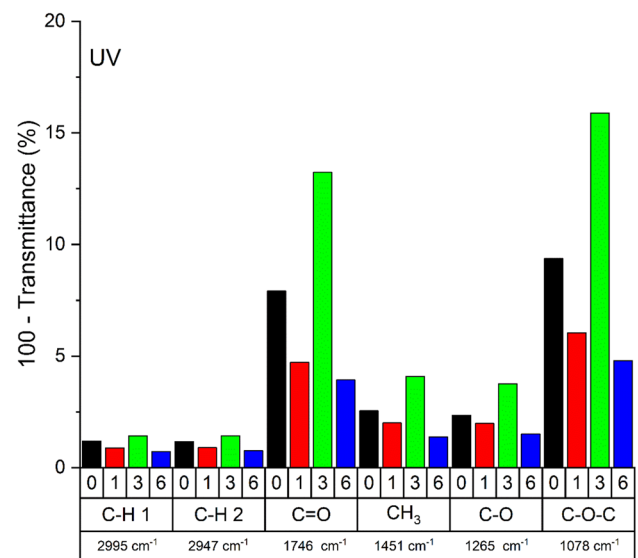


**Fig. 8** Absorbance of surface groups derived from FT-IR spectra for samples treated with UV. (0,1,3,6) on the X-axis indicate the treatment time in hours

### Drop Contour Analysis Results

The drop contour analysis findings indicate whether the polymer surface is hydrophilic or hydrophobic. The non-treated sample of PLA appears to have a hydrophilic surface and the values of the left and the right angles are 71.8° and 71.2°, respectively, as shown in Fig. 9. After the samples were treated either with Ultrasounds or with UVA irradiation their surfaces, even though they are still hydrophilic, in general they turned to be more hydrophobic than the reference, as shown at Table 1. These results seem to agree with the results obtained from the XPS characterization method, as it is explained above, when the samples are treated with ultrasonication there is an increase in the C-C bonds and a reduction of C-O or O-C=O bonds in the PLA. On the other hand, samples that have been treated with DBD

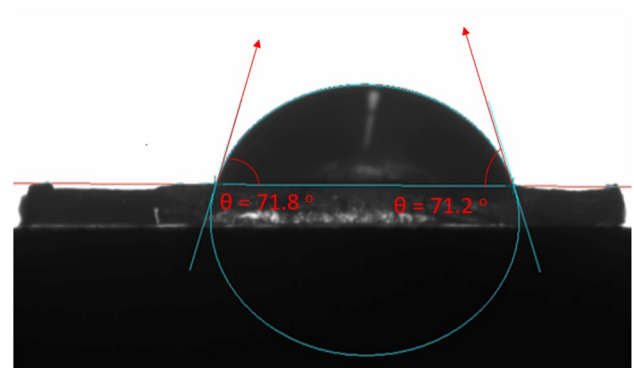


**Fig. 9** The non-treated (Reference) sample of PLA measured by DCA



**Table 1** Contact angle values from the drop contour analysis of the samples treated at different times and different methods

Treatment	Reference	UVA Irradiation			Ultrasounds at 20 kHz			Ultrasounds at 860 kHz		
		1 h	3 h	6 h	1 h	3 h	6 h	1 h	3 h	6 h
Angle 1 (°)	71.8	87.9	80.8	97.8	75.8	65.7	78.8	90.9	79.2	72.4
Angle 2 (°)	71.2	87.2	80.5	98.1	75.0	65.4	77.0	92.4	80.4	73.3

The chemical composition of the surface with treatment time

**Table 2** Contact angle values from the drop contour analysis of the samples treated with DBD plasma (Different PLA foil batch as compared to Table 1)

Treatment	Reference	Plasma			
		5 s	10 s	20 s	60 s
Angle 1 (°)	69.2	53.4	50.8	49.7	53.6
Angle 2 (°)	70.2	52.9	50.1	53.8	53.7

plasma appear to be more hydrophilic, as shown at Table 2. Once again, the results of DCA match the XPS results for the plasma treatment as the C–C bonds decrease and the O–C=O bonds increase. Therefore, the results of one treatment method cross the results of the other giving us the opportunity to adapt the surface chemical properties to different bacteria and enzymes.

### CLSM Results

This characterization method focuses more on the roughness and in general on the morphology of the surface. We, therefore, used it to collect more information about how the surface of our samples is changing morphologically, given by the values  $R_a$  and  $R_q$ .  $R_a$  expresses, as an absolute value, the difference in height of each point compared to the arithmetical mean of the surface and this parameter is used generally to evaluate surface roughness,  $R_q$  represents the root mean square value of ordinate values within the definition area and it is equivalent to the standard deviation of heights. Based on the results of CLSM we observe that the samples treated for 6 h at 20 kHz of Ultrasounds have a smoother surface than the Reference sample, but also from the samples treated for 1 or 3 h. The  $R_a$  value is decreased from 9.102 to 6.082 nm. Therefore, the smoother the surface gets one would expect that the surface is turning more hydrophobic. This theory agrees also with the DCA results showing that the surface is more hydrophobic as the contact angle is increased from 71.8° to 78.8°. Additionally, for the 860 kHz Ultrasound treatment a decrease of the  $R_a$  value for the samples treated for 3 h at 7.463 nm is observed. Then the value is increased again at 8.628 nm when the samples are treated for 6 h, which is close to the Reference. The DCA results also match these changes. However, during a measurement

the roughness is calculated only for a small part (in nm) of the whole surface of the sample, and although the values are the average of at least two measurements per sample, we do not consider that they represent the general aspect of the samples. More information about the CLSM results exist in the Supporting Information File.

### Bacteria Adhesion

From Fig. 10 it is obvious that the pre-treatment has a positive influence on the adhesion of *Pseudomonas Knackmussii*. This can be seen in the blueish color of the samples as well as the dark parts covering the PLA surface as compared to the reference. The surface percentage covered depends on the treatment method. Methods that oxidize the surface have a positive effect on the adhesion of the bacteria on the PLA surface. These results are in agreement with the conclusions of the XPS and DCA results on the surface chemistry as well as the hydrophilicity of the treated PLA samples.

### Discussion

As can be seen from the XPS and IR results, the time, at first glance, in which the samples are processed, does not play an important role. Large differences are observed after only 1 h of treatment. Therefore, we could assume that at time zero we have a "clean" untreated sample surface. Whereas the XPS investigations show that, the surface does not correspond to pure PLA, but it is slightly contaminated. Then we start treating the samples for one hour, during which changes are observed. The results of the three-hour analyses show that the sample surfaces again show significant differences from the reference but little difference from the sample after one hour. This is also true for samples treated for six hours. Especially the UVA treated samples show no major changes after 1 h. So, it seems that at least the ultrasonic treatments during the experiments cause the ablation of the top layer of the surface, resulting in a new modified PLA surface all the time. The IR results show, with two exceptions, that the PLA scaffold inside initially remains intact. It is not possible to say how much material can be removed with the respective treatment method now. However, the XPS results show that the changes start at the surface, and this

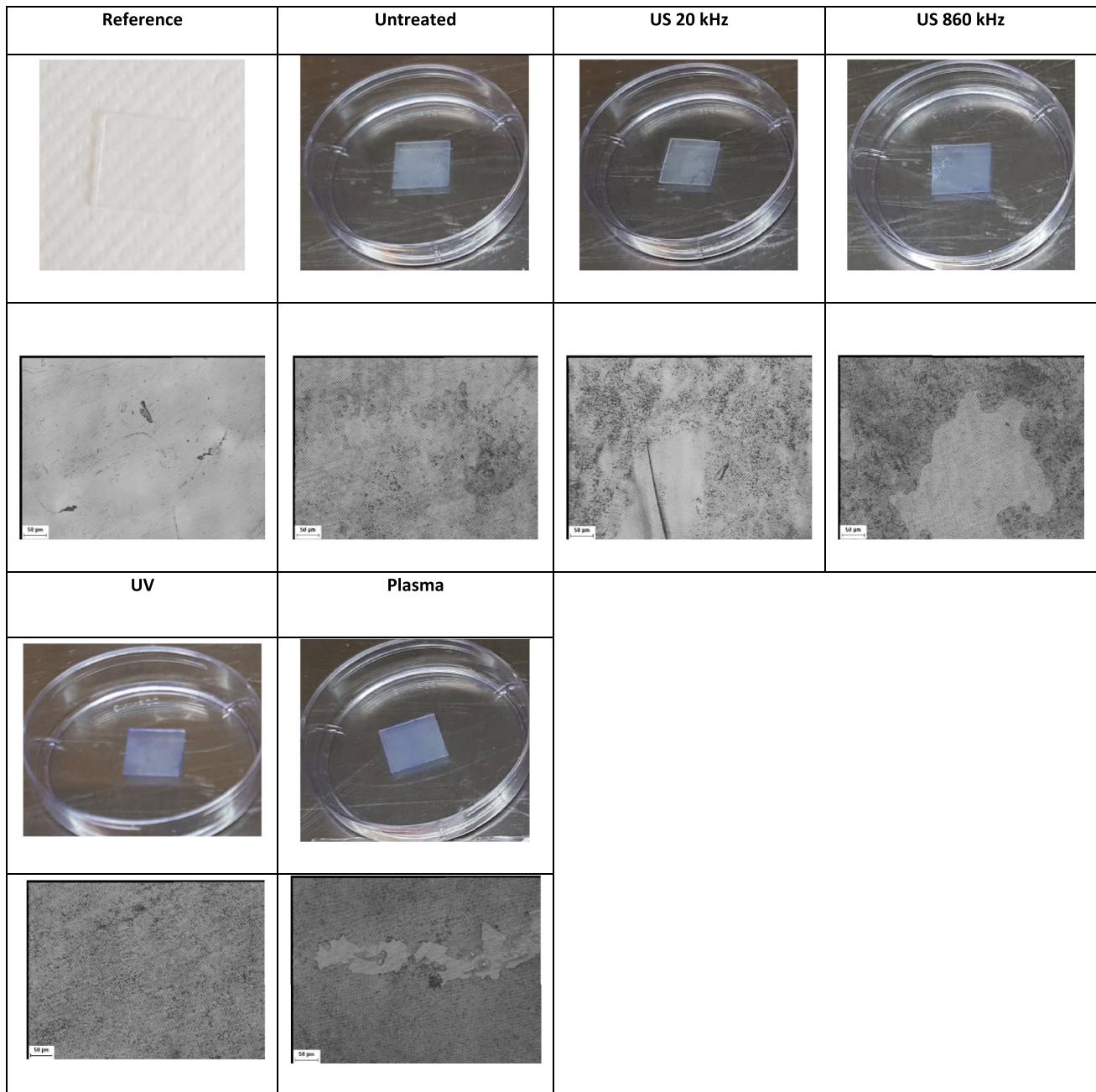


**Fig. 10** Pictures of the PLA samples after exposure to *Pseudomonas Knackmussii* showing the improved adhesion of the later as compared to the non-treated (Reference) sample of PLA

is where the differences in treatment type become apparent. The strongest changes were observed during treatment with 860 kHz and UV light. Here, we observe a strong increase in the C–C bonds on the surface. In contrast, treatment with 20 kHz leads to only marginal changes. Thus, the interaction of 20 kHz ultrasound with PLA in water seems to be less effective than that with 860 kHz as can be expected from the explanations on the way the different types of cavitation are acting on the PLA surface given in the introduction section.

The high frequency acts more in a chemical way and resembles the UV behaviour.

Samples treated at 20 kHz, show a slight increase in the C–C bonds and a reduction of C–O or O–C=O bonds in the PLA, without exhibiting a clear time dependence. It looks as if the C–C content increases up to the 3-h treatment and then falls again slightly which can be an indication of the mechanical cleaning effect of the low frequency US on the PLA surface.

Nitrogen was found again in the samples after a period of 3 h indicating a slow chemical incorporation process as we do not find indication for incorporated molecular nitrogen but only for chemical bonded nitrogen. In contrast to the low frequency US, the samples treated with 860 kHz exhibit an increase in the C–C bonds and a strong reduction in the C–O bonds, whereby the O–C=O bonds are stronger reduced. This behaviour is also observed in the interaction of UV radiation with the samples indicating a rather chemical interaction way of HFUS and UV and not mechanical as LFUS.

Comparing the UV data from the literature with the UV results presented here, a strong influence of the treatment environment is also evident. Significant differences are therefore observed between the samples where the treatment method was applied either in a wet environment or in air. Perhaps free radicals of the PLA surfaces are generated during hydrolysis and then water may transport the hydrolysis products away. This theory comes in agreement with literature [38] when PLA samples were treated via laser ablation in water.

In the plasma experiments despite the very short treatment times necessary, it is also observed that the treatment has an effect on the surface over time, but after a certain point, of approximately 20 s of treatment, the surface properties are very similar to the untreated surface. The plasma treatment, which took place in air, shows at first glance to have an opposite effect on the PLA. In this case, one could speak of an oxidation of the surface, which is associated with the relative increase in oxygen bonds compared to the C–C bonds. At second glance, however, only the C–C bonds are reduced, and the relative proportions approach the ratio of a pure PLA surface. This is also in good agreement with the literature [30]. Thus, one could speak of a cleaning effect. Drop Contour Analysis measurements support the XPS results. The samples with an increased amount of C–C bonds become more hydrophobic and the plasma treated samples with a lower amount of C–C bonds turn more hydrophilic.

As previously mentioned, all methods have an impact on the PLA structure in the surface. A first comparison of the methods was already made in our previous publication [20]. For the ultrasonic treatments, the different results can be attributed to the different energy input. At 20 kHz, the energy input is apparently not sufficient to split off a large number of characteristic molecular groups from the PLA or the radicals generated by the US are not reactive enough to change the PLA. The cavities created by the 860 kHz or the higher cavitation energy seem to be better at altering the PLA scaffold in this case. The stronger interaction not only decreases the oxygenated groups but also the roughness of the surface. In addition, at 860 kHz the larger number of tiny microbubbles compared to 20 kHz may have an important role. These bubbles do not implode (due to the small size,

surface tension, etc.) and show a strong oscillatory behaviour, which can scrub and change the surface of the sample.

From the UV experiments it can be concluded that the UV irradiation is more active than the ultrasonic irradiation, which may affect the cleavage of the C–O and O=C–O bonds. However, it does not affect the surface roughness because it has no mechanical effect. UV irradiation is therefore responsible for a purely chemical surface modification. The plasma interacts with the surface through various factors. The plasma itself consists of energetic and reactive particles (atomic and molecular), electrons and neutrons. In addition, the plasma is also a UV source. Cui and Brown explained the influence of plasma species [46] using the example of the interaction of an air-driven DBD with polypropylene. Reactive oxygen atoms have the strongest influence; they contribute the most to the oxidation of the surface. At the same time, high-energy plasma species can break C–C and C–H bonds, changing the surface morphology as it proceeds. This leads to the formation of additional reactive centers on the surface, which in turn can react with oxygen species. Moreover, they point out that oxidation processes, coupled with the removal of gaseous carbon species, such as CO and CO<sub>2</sub>, again lead to the exposure of intact layers. These mentioned processes can be transferred well to the interaction of Plasma with PLA also in comparison with the literature. The formation of more oxygen-containing groups in the PLA structure with the associated increased hydrophilicity is also observed.

In summary, it can be stated that the individual APOs change the PLA structure in the surface to a different extent, but for the comparison, the environment where the treatment takes place must also be included. This can subsequently influence the structural changes, e.g. through the removal of generated species.

## Conclusions

Considering all results of the influence of the pre-treatment methods together, it can be concluded that the changes of the PLA take place rather in the near-surface region.

The strongest changes were observed during treatment with 860 kHz and UV light. We observe a strong increase in the C–C bonds on the surface. In contrast, treatment with 20 kHz leads to only marginal changes. Ultrasonic treatments during the pretreatment experiments especially low frequency US cause the ablation of the top layer of the surface, resulting in a “fresh” PLA surface after 3 h, where we found the maximum change of the surface composition. The high frequency US acts more in a chemical way and resembles the UV behaviour.

Nitrogen was found in the ultrasonicated samples after a period of 3 h indicating a slow chemical incorporation

process as we do not find indication for incorporated molecular nitrogen but only for chemical bonded nitrogen.

With plasma we observe an oxidation of the surface, which, however, lies more on the reduction of the C–C bonds relative to the C–O and C=O bonds.

Finally, we tested pre-treated PLA foils regarding a possible improved adhesion of bacteria strains and found in the example of the *Pseudomonas knackmussii* strain that depending on the pre-treatment method the adhesion has been substantially improved.

**Supplementary Information** The online version contains supplementary material available at <https://doi.org/10.1007/s10924-022-02608-w>.

**Acknowledgements** We are indebted to Dr. Ramesh Babu Padamati (AMBER & BiOrbic Research Centre; School of Chemistry, Trinity College Dublin) as well as to Assoc. Professor Matina Vougiouka (School of Chemical Engineering, National Technical University of Athens, Greece) for providing PLA foils.

**Authors Contributions** GS, CK, and CA contributed to the study conception and design. Material preparation, data collection and analysis were performed by CK, GS, NP, OH, AG and PP. Quality control of the data and analyses were performed by GS, CK and CA. The first draft of the manuscript was written by CK and CA and all authors commented on previous versions of the manuscript. All authors read and approved the final manuscript.

**Funding** Open Access funding enabled and organized by Projekt DEAL. The authors declare that this study has been partly funded from the European Union's Horizon 2020 research and innovation program under grant agreement number 870292 (BioICEP).

## Declarations

**Conflict of interest** The authors declare that they have no known competing interests.

**Open Access** This article is licensed under a Creative Commons Attribution 4.0 International License, which permits use, sharing, adaptation, distribution and reproduction in any medium or format, as long as you give appropriate credit to the original author(s) and the source, provide a link to the Creative Commons licence, and indicate if changes were made. The images or other third party material in this article are included in the article's Creative Commons licence, unless indicated otherwise in a credit line to the material. If material is not included in the article's Creative Commons licence and your intended use is not permitted by statutory regulation or exceeds the permitted use, you will need to obtain permission directly from the copyright holder. To view a copy of this licence, visit <http://creativecommons.org/licenses/by/4.0/>.

## References

- Andrady AL, Neal MA (2009) Applications and societal benefits of plastics. *Phil Trans Royal Soc B* 364(1526):1977–1984. <https://doi.org/10.1098/rstb.2008.0304>
- Worm B, Lotze HK, Jubinville I, Wilcox C, Jambeck J (2017) Plastic as a persistent marine pollutant. *Annu Rev Environ Resour* 42(1):1–26. <https://doi.org/10.1146/annurev-envir-102016-060700>
- World Economic Forum (2016). The new plastics economy: Rethinking the future of plastics. World Economic Forum. [http://www3.weforum.org/docs/WEF\\_The\\_New\\_Plastics\\_Economy.pdf](http://www3.weforum.org/docs/WEF_The_New_Plastics_Economy.pdf).
- Law KL (2017) Plastics in the marine environment. *Ann Rev Mar Sci* 9(1):205–229. <https://doi.org/10.1146/annurev-marine-010816-060409>
- Zhuang W et al (2008) Preparation, characterization, and properties of TiO<sub>2</sub>/PLA nanocomposites by in situ polymerization. *Polym Compos*. <https://doi.org/10.1002/pc.20658>
- von der Esch E, Lanzinger M, Kohles AJ, Schwaferts C, Weisser J, Hofmann T, Glas K, Elsner M, Ivleva NP (2020) *Front Chem* 8:169. <https://doi.org/10.3389/fchem.2020.00169>
- Sun C, Wei S, Tan H, Huang Y, Zhang Y (2022) Progress in upcycling poly(lactic acid) waste as an alternative carbon source: A review. *Chem Eng J* 446:136881
- Nampoothiri KM, Nair NR, John RP (2010) An overview of the recent developments in polylactide (PLA) research. *Bioresour Technol* 101:8493–8501. <https://doi.org/10.1016/j.biortech.2010.05.092>
- Morohoshi T, Ogata K, Okura T, Sato S (2018) Molecular characterization of the bacterial community in biofilms for degradation of poly(3-hydroxybutyrate-co-3-hydroxyhexanoate) films in seawater. *Microbes Environ* 33:19–25
- Haider TP, Völker C, Kramm J, Landfester K, Wurm FR (2019) Plastics of the future? the impact of biodegradable polymers on the environment and on society. *Angew Chem Int Ed* 58:50–62. <https://doi.org/10.1002/anie.201805766>
- Sabee M, Saddiq MM, Kamalaldin N, Yahaya B, Hamid ZA (2016) Characterization and in vitro study of surface modified PLA microspheres treated with NaOH. *J Polym Mater* 33:191–200
- Zafar MT, Maitia SN, Ghosh AK (2016) Effect of surface treatments of jute fibers on the microstructural and mechanical responses of poly(lactic acid)/jute fiber biocomposites. *Waste Manage*. <https://doi.org/10.1039/C6RA17894D>
- Mat Yasin N, Akkermans S, Van Impe JFM (2022) Enhancing the bio-degradation of (bio)plastic through pretreatments: A critical review. *Waste Manage* 150:1–12. <https://doi.org/10.1016/j.wasman.2022.06.004>
- Fridman A (2008) *Plasma Chemistry*. Cambridge University Press, Cambridge
- Dong D, Tasaka S, Inagaki N (2001) Thermal degradation of monodisperse polystyrene in bean oil. *Polym Degrad Stab* 72(2):345–351. [https://doi.org/10.1016/S0141-3910\(01\)00031-3](https://doi.org/10.1016/S0141-3910(01)00031-3)
- Fotopoulou K, Karapanagioti H (2017) Degradation of Various Plastics in the Environment. In: Takada H, Karapanagioti HK (eds) *Hazardous Chemicals Associated with Plastics in the Marine Environment*. Springer, Cham
- Suslick K, Choe SB, Cichowlas A et al (1991) Sonochemical synthesis of amorphous iron. *Nature* 353:414–416. <https://doi.org/10.1038/353414a0>
- Mason T, Lorimer JP (2002) *Applied Sonochemistry: Uses of Power Ultrasound in Chemistry and Processing*. Wiley-VCH, NJ
- Gedanken A (2004) Using sonochemistry for the fabrication of nanomaterials. *Ultrason Sonochem* 11(2):47–55. <https://doi.org/10.1016/j.ultsonch.2004.01.037>
- Gogate PR, Prajapat AL (2015) Depolymerization using sonochemical reactors: A critical review. *Ultrason Sonochem* 27:480–494. <https://doi.org/10.1016/j.ultsonch.2015.06.019>
- Pasupuleti S, Madras G (2010) Ultrasonic degradation of poly(styrene-co-alkyl methacrylate) copolymers. *Ultrason Sonochem* 17:819–826. <https://doi.org/10.1016/j.ultsonch.2010.02.003>
- Sourkouni G, Kalogirou C, Moritz P, Gösde A, Pandis PK, Höfft O, Vougiouka S, Zorpas A, Argiris C (2021) *Ultrason Sonochem* 76:105627. <https://doi.org/10.1016/j.ultsonch.2021.105627>

23. Ranby B (1989) Photodegradation and photo-oxidation of synthetic polymers. *J Anal Appl Pyrolysis* 15:237–247. [https://doi.org/10.1016/0165-2370\(89\)85037-5](https://doi.org/10.1016/0165-2370(89)85037-5)
24. Singh B, Sharma N (2008) Mechanistic implications of plastic degradation. *Polym Degrad Stab* 93:561–584. <https://doi.org/10.1016/j.polymdegradstab.2007.11.008>
25. Chaozong Liu, Naiyi Cui, Norman M. D Brown, Brian J Meenan, Effects of DBD plasma operating parameters on the polymer surface modification, *Surf Coat Technol*, doi: <https://doi.org/10.1016/j.surfcoat.2004.01.024>.
26. Ren C-S, Wang K, Nie Q-Y, Wang D-Z, Guo S-H (2008) Surface modification of PE film by DBD plasma in air. *Appl Surf Sci* 255:3421–3425. <https://doi.org/10.1016/j.apsusc.2008.09.064>
27. Sarasua J.-R., N. Lopez Rodriguez, A. López Arraiza, and E. Meaurio (2005) *Macromolecules* 38, 8362–8371
28. Sarasua J.-R., A. López Arraiza, P. Balerdi, I. Maiza, Crystallization and Thermal behaviour of optically pure polylactides and their blends, *J. Mater. Sci* 40 (2005) 1855–1862
29. Son AY, Oh YA, Kim SH, Min SC (2016) *J Food Sci* 81:E86–E95
30. Engelhard, M.H., T.C.Droubay, Y.Du, X-Ray Photoelectron Spectroscopy Applications, in *Encyclopedia of Spectroscopy and Spectrometry* (3rd Edition), Pages 716–724 <https://doi.org/10.1016/B978-0-12-409547-2.12102-X>
31. Storp S (1985) Radiation damage during surface analysis. *Spectrochim Acta, Part B* 40B(5–6):745–756
32. G. Beamson, D. Briggs, High Resolution XPS of Organic Polymers: The Scienta ESCA300 Database, John Wiley & Sons Ltd (1992), 10.1002/ [Titel anhand dieser DOI in Citavi-Projekt übernehmen] pi.1994.210330424.
33. Scofield JH (1976) Hartree-Slater subshell photoionization cross-sections at 1254 and 1487 eV. *J Electron Spectrosc Relat Phenom* 8(2):129–137. [https://doi.org/10.1016/0368-2048\(76\)80015-1](https://doi.org/10.1016/0368-2048(76)80015-1)
34. Yeh JJ, Lindau I (1985) Atomic subshell photoionization cross sections and asymmetry parameters:  $1 \leq Z \leq 103$ . *At Data Nucl Data Tables* 32(1):1–155. [https://doi.org/10.1016/0092-640X\(85\)90016-6](https://doi.org/10.1016/0092-640X(85)90016-6)
35. Carlsson K, Danielsson PE, Lenz R, Liljeborg A, Majlöv L, Åslund N (1985) Three-dimensional microscopy using a confocal laser scanning microscope. *Opt Lett* 10:53–55
36. Paddock SW (2000) Principles and practices of laser scanning confocal microscopy. *Mol Biotechnol* 16:127–149. <https://doi.org/10.1385/MB:16:2:127>
37. Skinner FK, Rotenberg Y, Neumann AW (1989) Contact angle measurements from the contact diameter of sessile drops by means of a modified axisymmetric drop shape analysis. *J Colloid Inter Sci* 130:25–34. [https://doi.org/10.1016/0021-9797\(89\)90074-X](https://doi.org/10.1016/0021-9797(89)90074-X)
38. Spelt JK, Rotenberg Y, Absolom DR, Neumann AW (1987) Sessile-drop contact angle measurements using axisymmetric drop shape analysis. *Coll Surf* 24(2–3):127–137. [https://doi.org/10.1016/0166-6622\(87\)80345-1](https://doi.org/10.1016/0166-6622(87)80345-1)
39. Tiernan H, Byrne B, Kazarian SG (2020) *Spectrochimica Acta Part A* 241:118636. <https://doi.org/10.1016/j.saa.2020.118636>
40. Shakesheff KM, Evora C, Soriano II, Langer R (1997) The adsorption of poly(vinyl alcohol) to biodegradable microparticles studied by X-Ray photoelectron Spectroscopy (XPS). *J Colloid Interface Sci* 185(2):538–547. <https://doi.org/10.1006/jcis.1996.4637>
41. Krtouš Z, Hanyková L, Krakovský I, Nikitin D, Pleskunov P, Kylián O, Sedlářková J, Kousal J (2021) Structure of plasma (re) polymerized polylactic acid films fabricated by plasma-assisted vapour thermal deposition. *Materials* 14:459. <https://doi.org/10.3390/ma14020459>
42. De Geyter N, Morent R, Desmet T, Trentesaux M, Gengembre L, Dubruel P, Leys C, Payen E (2010) Plasma modification of polylactic acid in a medium pressure DBD. *Surf Coat Technol* 204(20):3272–3279. <https://doi.org/10.1016/j.surfcoat.2010.03.037>
43. Laput O, Vasenina I, Salvadori M-C, Savkin K, Zuza D, Kurzina I (2019) *J Mater Sci* 54:11726–11738. <https://doi.org/10.1007/s10853-019-03693-4>
44. Song AY, Oh YA, Roh SH, Kim JH, Min SC (2016) Cold oxygen plasma treatments for the improvement of the physicochemical and biodegradable properties of polylactic acid films for food packaging. *J Food Sci* 81(1):E86–E96. <https://doi.org/10.1111/1750-3841.13172>
45. Ikada E (1997) *J Photopol Sci Technol* 10(2):265–270. <https://doi.org/10.2494/photopolymer.10.265>
46. G. Socrates, 2004, *Infrared and Raman Characteristic Group Frequencies*, 3. Ed., John Wiley & Sons, LTD.
47. Wei J, Luo Yiming Yu, Jian LB, Minglie Hu, Chai Lu, Chingyue W (2015) Effects of high-repetition-rate femtosecond laser micromachining on the physical and chemical properties of polylactide (PLA). *Opt Express* 23:26932–26939. <https://doi.org/10.1364/OE.23.026932>
48. Nai-Yi Cui and Norman M.D. Brown, Modification of the surface properties of polypropylene (PP) film using an air dielectric barrier discharge plasma, *Appl Surf Sci*, 189 (2002) 31–38

**Publisher's Note** Springer Nature remains neutral with regard to jurisdictional claims in published maps and institutional affiliations.